



Working Load Measurement and Analysis of Bolted Joint under Off-road Vehicle Operation

Soichi Hareyama and Ken-ichi Manabe Tokyo Metropolitan University

Citation: Hareyama, S. and Manabe, K.-I., "Working Load Measurement and Analysis of Bolted Joint under Off-road Vehicle Operation," SAE Technical Paper 2018-01-1234, 2018, doi:10.4271/2018-01-1234.

Abstract

In this study, we propose a method of measuring and analyzing the load on bolted joints used in a machine under off-road vehicle operation. Working load measurement under actual machine operation and the results of its analysis are shown as load frequency diagrams. An example of the

measurement analysis of a load (three types of load: axial force, bending moment, and torsional torque) added to a bolted joint shank during actual machine operation is shown. In this paper, we describe how to apply the results of load analysis to the load condition at the design and experimental development stages.

Introduction

In heavy-duty off-road vehicles used as industrial and construction machinery, very severe loads are applied to bolted joints, which tighten structural strength members, and thus close attention must be paid to their strength and self-loosening. SAE Fatigue Design Handbook [1] shows two important steps, namely, the "Load Estimate step in the DESIGN STAGE" and the "Service Load Evaluation step in the EXPERIMENTAL DEVELOPMENT STAGE". The load condition is necessary for both the design and experimental conditions, and this is very important information for realizing the above-mentioned concurrent multiple design concept.

The main types of bolt problems are fatigue fracture and self-loosening, the causes of which are design-based faults and insufficient clamping force (tightening torque), respectively. Several design analyses on loads applied to bolted joints have been carried out. Bickford [2] proposed a fundamental concept and guidelines for the fatigue failure of bolted joints. Japan Research Institute for Screw Threads and Fasteners (JFRI) [3] published the "Analysis and Design for Bolted Joints". VDI 2230 [4] provided design information on the durability of bolted joints.

Gadgets, machines, and spacecraft may not even exist without screws and bolts. Although screws and bolts are machine parts based on the simple principle of a wedge and a spiral and have been used for more than 2000 years, problems such as poor bolting, self-loosening, and insufficient strength occur even today.

Concerning these problems, several papers were analyzed by the authors. Firstly, the optimum tightening condition of a bolted joint used in a machine is defined as the state in which the joint is tightened with sufficiently high clamping force (axial tension) to be free from breakage and loosening by any external force during machine operation [5-8].

Regarding the prevention of fatigue breakage, Kumar [9] and Ellis et al. [10] investigated fatigue life prediction. The authors also showed a method for the lifetime evaluation of fatigue failure and the analysis of loads applied to bolted joints [11]. Much research into the effect of self-loosening prevention measures has been carried out using self-loosening test machines. In our previous paper [12], we proposed a loosening lifetime prediction and residual clamping force estimation method for bolt loosening during actual machine operation. The proposed technique can be used to predict in the early stage of machine development, the decrease in clamping force after a long period of machine operation by comparing these predictions with measurements in actual machines. Various studies have been conducted on the problems of bolted joints and the elucidation of the self-loosening mechanism shown below. In particular, the research of Junker and Williams provided many suggestions on the mechanism and the laboratory loosening test method [13,14].

Concerning failure analysis, Baggerly [15] investigated the hydrogen embrittlement of a wheel bolt. Fukuoka et al. [16] analyzed the cyclic stress amplitude of wheel bolts for large vehicles. Thus, problems with bolted joints can be divided roughly into fatigue breakage, hydrogen embrittlement, and self-loosening.

In particular, research on the fatigue strength of bolted joints has led to the proposal of many methods of lifetime prediction. JFRI [17] obtained the cooperation of several universities and companies and carried out numerous investigations on fatigue. Weber et al. [18] examined the fatigue limit of high-strength bolts. Minguez and Vogwell [19] investigated the effect of torque tightening on the fatigue strength of bolted joints.

In this paper, a method of analyzing loads applied to bolted joints was investigated, including the case of multiple

loads. Moreover, measurement method using strain gauges and equations for conducting analysis are proposed. By taking a construction machine (wheel loader) as an example, the load actually applied to bolted joints during machine operation is analyzed. The effectiveness of the proposed method was proved by showing that accurate fatigue strength estimation was possible using the posited relationship between loads and stresses.

Analysis of Loads Applied to Bolted Joints

In the design of bolted joints, their structure is generally devised such that the load condition of the bolts is simplified using knock pins or spigot joints that join with a flange joint, so that either the shearing force or tangential force can be neglected. Therefore, in bolted joints to which an axial force (tension), bending moment, and torsional torque are applied, it is possible to measure and analyze the loads in accordance with the methods described below.

Measurement of Axial Force (Tension)

Figure 1 shows two axial force measurement methods. The first is the bolt gauge method, as shown in Fig. 1-(a), with a normal hexagon head bolt and a hub bolt, for example. The axial force is obtained from Equation (1). The second is the two-strain-gauge method, as shown in Fig. 1-(b), with a hub bolt, for example. The axial force is obtained from Equation (2).

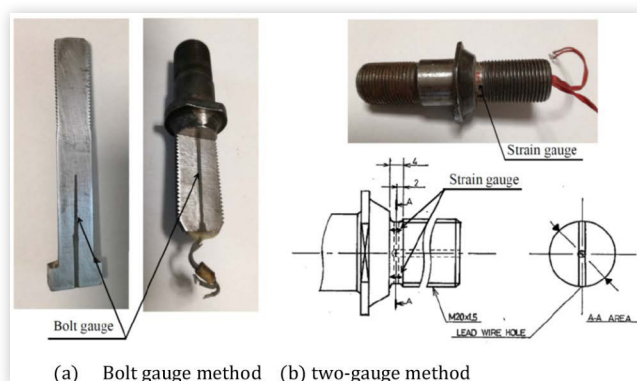
$$P_b = \frac{E \cdot A_b}{2} (\varepsilon_b) \dots \dots \quad (1)$$

$$P = \frac{E \cdot A_r}{2} (\varepsilon_{AII} + \varepsilon_{CII}) \dots \dots \quad (2)$$

Here,

P_b : Axial force (tension) at point measured by bolt gauge method

FIGURE 1 Axial force measurement method using strain gauge (a) Bolt gauge method (b) two-gauge method



P : Axial force at point measured by two-gauge method (the strains measured using uniaxial strain gauges on both sides are denoted as ε_{AII} and ε_{CII})

E : Modulus of longitudinal elasticity of bolt shank

A_r : Sectional area of bolt shank at measured point

Measurement of Bending Moment and Torsional Torque

Figure 2 shows the positions of strain gauges bonded to a bolt shank to measure loads as well as the relationship between these loads. Each load applied to a bolted joint is assumed to act along or around the bolt axis. As shown in the figure, the strain gauges at measured points are arranged so that three orthogonal axis strain gauges are bonded at A and C, a central gauge coincides with the bolt axis, and uniaxial strain gauges bonded at B and D are parallel with the bolt axis. The strains measured by the three orthogonal axis strain gauges I, II, and III at A, for example, are denoted as ε_{AI} , ε_{AII} , and ε_{AIII} , and those measured by uniaxial strain gauges at B and D are denoted as ε_{BII} and ε_{DII} , respectively. Then, the loads applied to the bolted joint are characterized as follows.

$$M_x = \frac{E \cdot Z_b}{2} (\varepsilon_{AII} - \varepsilon_{CII}) \dots \dots \quad (3)$$

$$M_y = \frac{E \cdot Z_b}{2} (\varepsilon_{BII} - \varepsilon_{DII}) \dots \dots \quad (4)$$

$$T_z = \frac{G \cdot Z_p}{2} \{ (\varepsilon_{AIII} - \varepsilon_{CIII}) + (\varepsilon_{BII} - \varepsilon_{DII}) \} \dots \dots \quad (5)$$

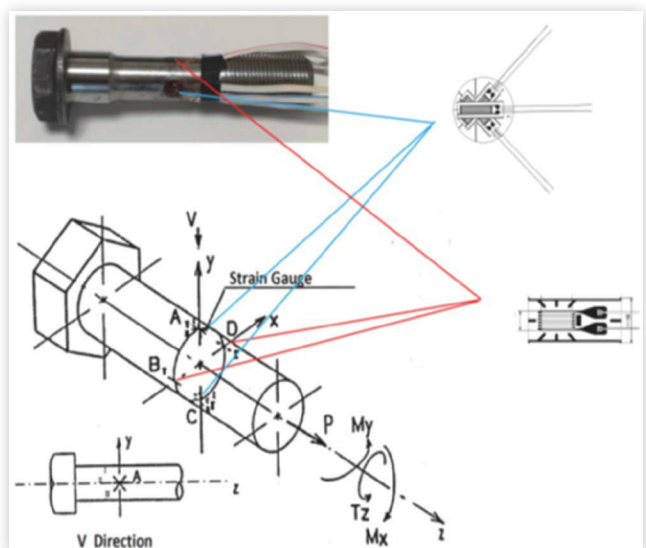
Here,

M_x : Bending moment around x-axis at measured point

M_y : Bending moment around y-axis at measured point

T_z : Torsional torque around z-axis at measured point

FIGURE 2 Relationship between the measurement locations of strain gauges and loads for bending moment and torsional torque



Z_b : Section modulus of bolt shank

Z_p : Polar modulus of section of bolt shank

G : Modulus of transverse elasticity of bolt shank

The composite bending moment of the bending moments M_x and M_y and the direction of the operational axis of this composite moment are given below.

$$M_e = \sqrt{M_x^2 + M_y^2}$$

$$= \frac{E \cdot Z_b}{2} \sqrt{(\varepsilon_{AII} - \varepsilon_{CII})^2 + (\varepsilon_{BII} - \varepsilon_{DII})^2} \dots \quad (6)$$

$$\tan \alpha_M = \frac{M_y}{M_x} = \frac{(\varepsilon_{BII} - \varepsilon_{DII})}{(\varepsilon_{AII} - \varepsilon_{CII})} \dots \quad (7)$$

Here,

M_e : Composite bending moment

α_M : Angle from x-axis to operational axis of composite bending moment (in counterclockwise direction)

Application to Load Measurement in an Actual Machine

The fundamental concept of the measurement of a load applied to bolted joints has been described. It was confirmed by simple experiments that this method enables the analysis of multiple separate applied loads with high accuracy. In this section, the results of applying this load analysis method to an actual machine are also described.

Test Pieces and Experimental Conditions

Figure 3-a) shows an axle of a construction machine (wheel loader). The bolts analyzed here were setting bolts to fix a hub to the central axis of a planetary gear-type reduction

FIGURE 3 Tested structure and set bolt (actual machine)

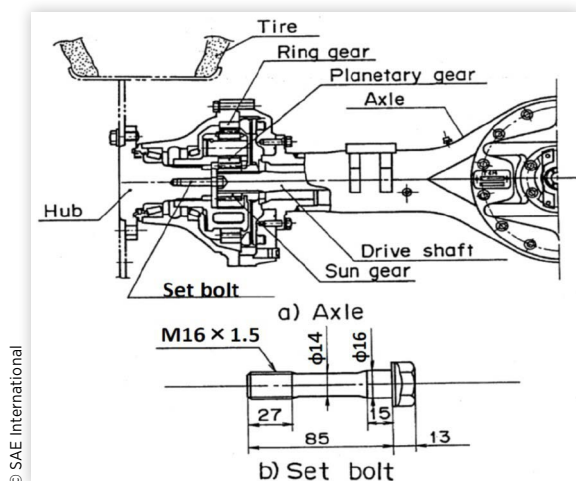
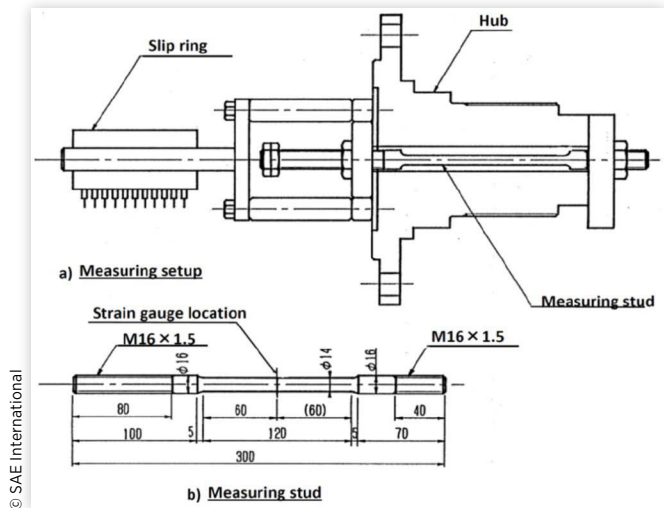


FIGURE 4 Load-measuring apparatus and measurement stud



component. As the hub is the rotating part, the set bolt is considered to be subjected to multiple loads such as torsional torque and an axial force. Figure 3-b) shows the dimensions of the set bolt. To analyze loads applied to the bolt with this simple structure, measurement was carried out using a stud with a cross section as shown in Fig. 4-a). Figure 4-b) shows the dimensions of the measurement stud. Figure 5 shows a photograph of the load-measuring apparatus and measurement stud.

Operation load measurement was carried out during a cycle of shoveling and dumping operations as shown in Figs. 6 and 7, which is a typical working pattern for a wheel loader.

FIGURE 5 Photograph of load-measuring apparatus and measurement stud



FIGURE 6 Actual machine operation at test site



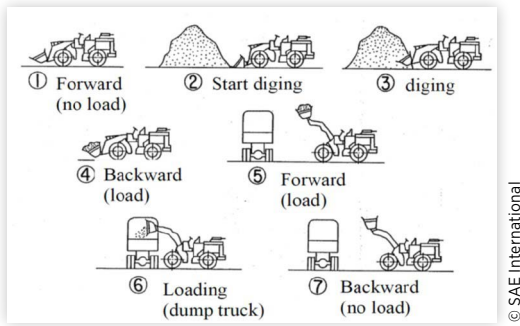
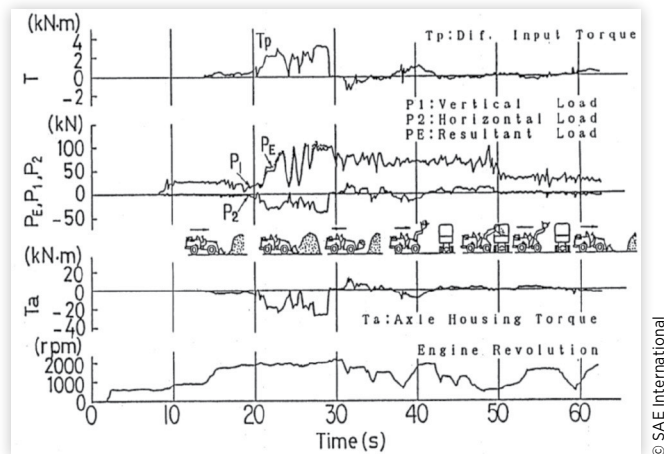
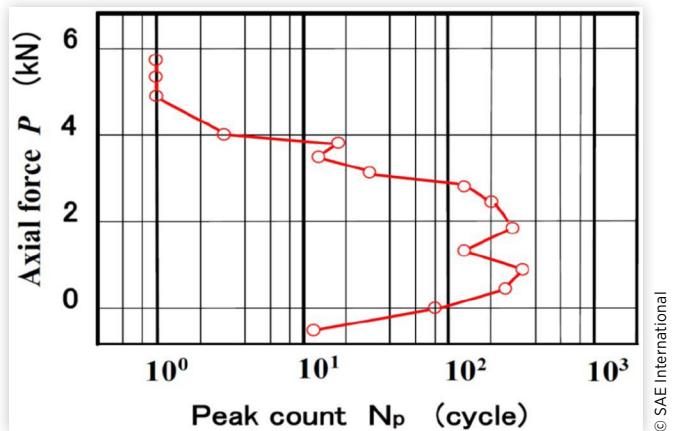
FIGURE 7 Shoveling and dumping operations**FIGURE 8** Load pattern (one cycle) of the axle part during shoveling and dumping

Figure 8 shows a load pattern (one cycle) of the axle part during shoveling and dumping. The graph shows the measured pattern of the load applied to tires in one operation cycle. T_p shows input torque wave of differential gear. P_1 and P_2 show vertical and horizontal load which wheel loader tier were affected, respectively. PE shows composite (resultant) tier load of the tier load P_1 and P_2 . T_a shows axle housing torque as correspond to drive shaft torque (c.f. Fig. 3). These load analysis results were used for component and machine level test condition. It is necessary to analyze the fatigue strength to estimate data over a long period, and therefore loads during repeated cycles were measured several times.

Load Peak Frequency Analysis in Case of Axial Force

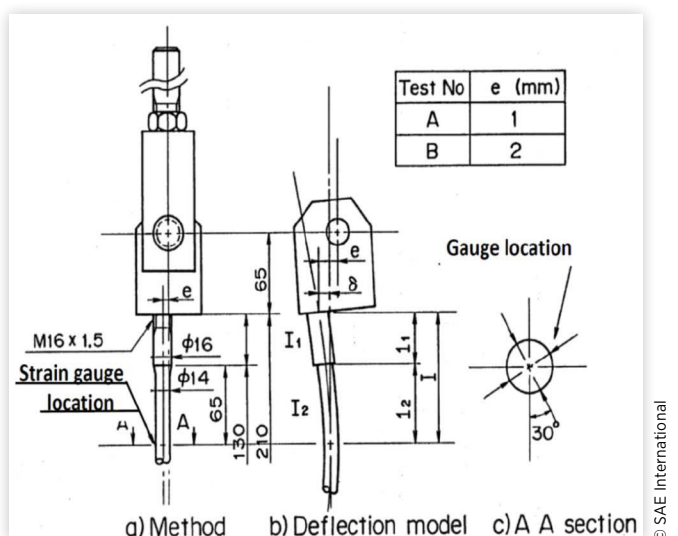
Load estimation is carried out using Equations (1) and (2), where the shearing force and tangential force are assumed to be negligible. Measured loads were analyzed using a data processing device. Figure 9 shows the measurement results of the load distribution (axial force) as a load frequency diagram.

FIGURE 9 Load distribution (axial force)

Load Peak Frequency Analysis in Case of Bending Moment

The axial force and bending moment were measured by attaching strain gauges to the center of a stepped stud constructed for load measurement, as shown in Fig. 4, and placing it in the vertically symmetrical tensile testing machine shown in Fig. 10-a). This stud is also used in load measurement during the actual operation of a machine as mentioned later. A bending moment is applied by setting the eccentricity “ e ” between the axis of the tensile testing machine and the stud. This experimental apparatus can be configured as shown in Fig. 10-b), where an eccentric tensile load is applied to a rod. By neglecting the effect of the processing precision of the supporting part of the stud, the bending moment M_c can be expressed using the equations below.

$$M_c = P(e - \delta) \dots \quad (8)$$

FIGURE 10 Experimental apparatus for axial force and bending moment

$$\delta = \frac{\alpha_1 \cdot e}{\alpha_1 \cos \alpha_1 l_1 \cdot \cos \alpha_2 l_2 - \alpha_1 \sin \alpha_1 l_1 \cdot \sin \alpha_2 l_2} - e \quad (9)$$

$$\text{Here, } \alpha_1 = \frac{P}{EI_1}, \alpha_2 = \frac{P}{EI_2},$$

where

I_1 : geometrical moment of inertia of supporting part of stud,

I_2 : geometrical moment of inertia of measuring part of stud.

Figure 11 shows the composite bending moment M_e , calculated with Equation (6) using the values obtained from the above equations based on the strain gauge measurements, with the results calculated with Equation (8). They generally agree with each other, but there is a rather large difference between certain values. This is considered to be due to inaccuracy in the finishing of the test piece and the backlash of the threads.

Figure 12 shows the measured axial force (tension) and the angle of the bending moment axis. It is shown that the applied load can be measured with high accuracy by measuring the axial tension. The accuracy of the measurement of the angle of the bending moment axis, α_M , increases with the applied load. This experiment was carried out for a stud set 30 deg. from the axis of the bonded strain gauges, as shown in Fig. 10-c).

The above results show that this measurement method enables separate and accurate analysis of the axial force (tension) and bending moment in the case where both are applied at the same time. Figure 13 gives the numbers of occurrences of load peaks of the bending moment as a load frequency diagram.

FIGURE 11 Calculated and experimental results for bending moment

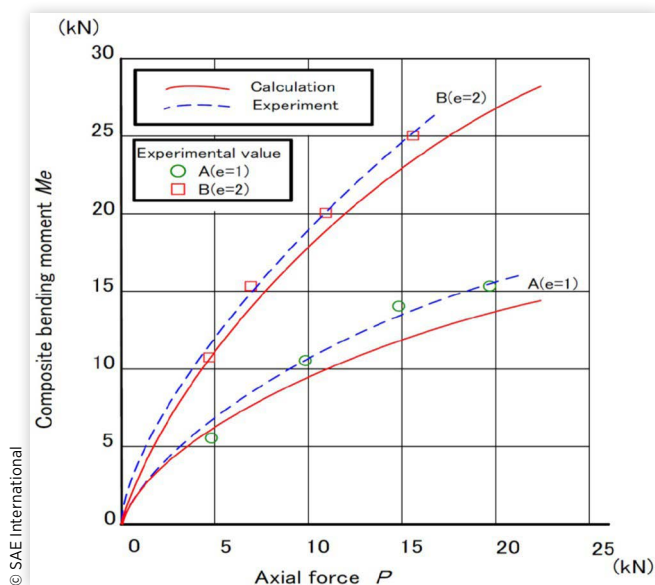


FIGURE 12 Axial force (tension) and angle of bending moment axis

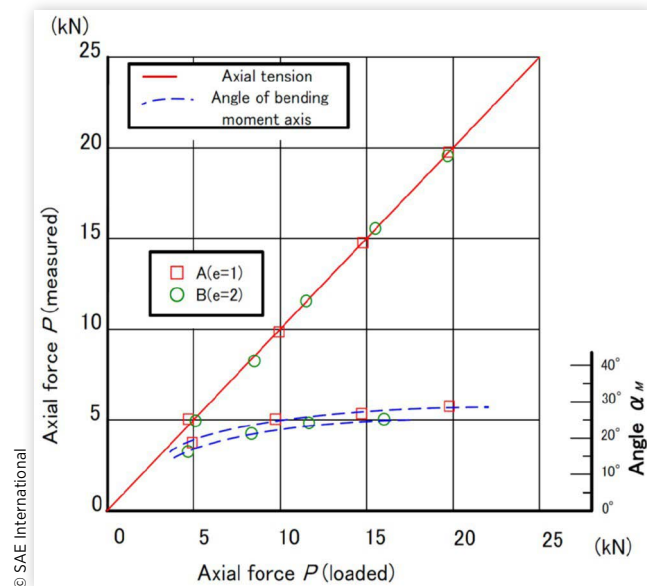
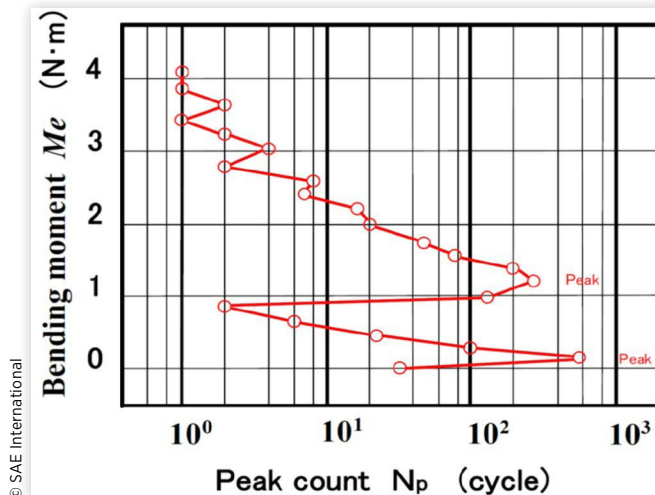
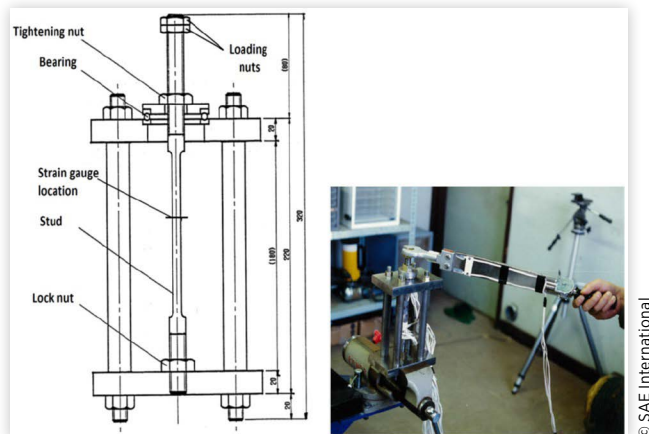
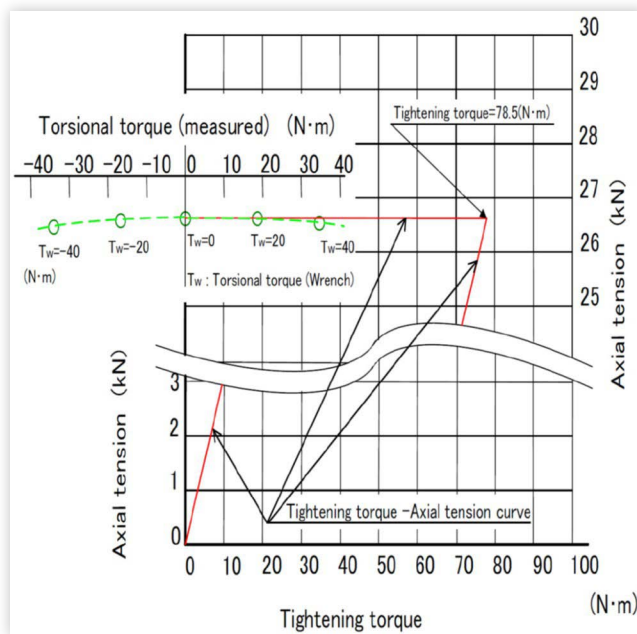


FIGURE 13 Load distribution (bending moment)



Load Peak Frequency in Case of Torsional Torque [Axial Force (Tension) and Torsional Torque]

It was determined whether axial force (tension) and torsional torque can be separately measured with accuracy in the case where both are applied at the same time by measuring changes in stress, where the axial force is initially applied to a stud to which torsional torque is being applied, using the experimental apparatus shown in Fig. 14. The experiment was carried out by adding torsional torque with a loading nut after twisting a tightening nut with a torque of 78.5 Nm.

FIGURE 14 Experimental apparatus for axial force and torsional torque**FIGURE 15** Experimental results for axial force (tension) and torsional torque (change in the axial tension with the torsional torque)

Strain was measured at the central part of the stud similarly to in the case shown in Fig. 1. Figure 15 shows the experimental results; hardly any change in the axial tension was observed with the addition of torsional torque after tightening. This means that this measurement method also enables the analysis of these two factors with sufficient accuracy in the case where both an axial force (tension) and torsional torque are applied. The same should hold for the case of a bending moment and a torsional torque applied at the same time, considering the relationship between the axial strain and the shearing strain. A possible reason why the torsional torque measured from the strain gauges in the stud is slightly lower than it should be, namely, 85% of the actual loaded torsional torque, is that there were losses due to friction at the bearing.

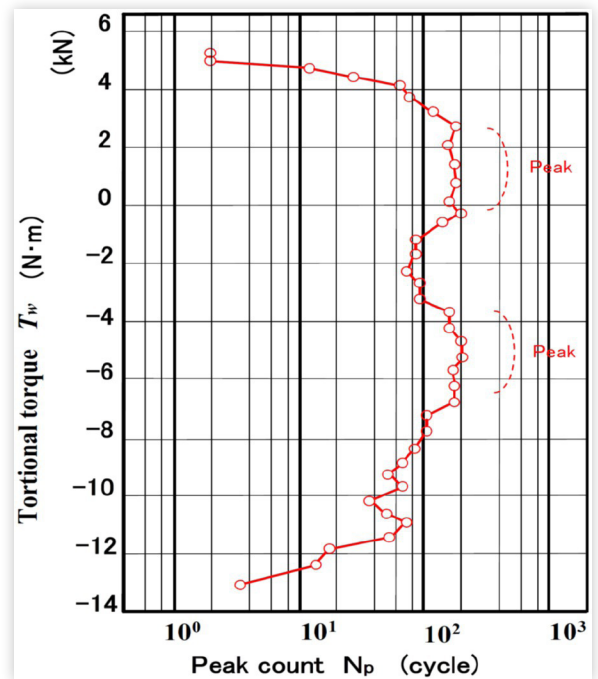
FIGURE 16 Load distribution (torsional torque)

Figure 16 shows the numbers of occurrences of load peaks of torsional torque applied to the bolt joint as a load frequency diagram. The load peak distributions of both the bending moment in Fig. 13 and the torsional torque seem to have two peaks. This is considered to result from the superposition of respective load peaks during shoveling and traveling work and in forward and reverse motion.

Relationship between Load and Stress

In this experiment, a load-measuring stud was used instead of an actual bolt; therefore, it is necessary to estimate the load and stress of an actual bolt from the measurements of the stud. When an external force W_a is applied to the bolted joint part of the load-measuring stud, the relationship between the axial tension generated in the stud, P_A , and the external force is as follows.

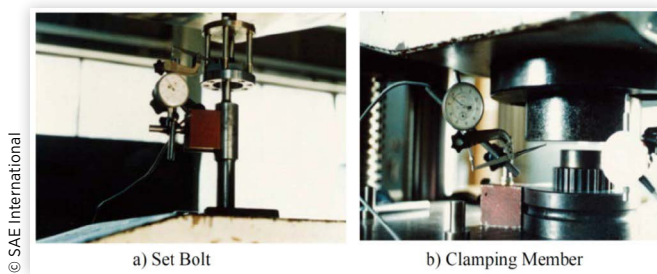
$$P_A = \phi_T \cdot W_a \quad (10)$$

Here,

ϕ_T : Stiffness constant factor of bolted joint part of load-measuring stud

Figure 17 shows a photograph of the spring constant measurement apparatus, Fig. 17-a) and Fig. 17-b) show spring constant-measuring apparatus of set bolt and clamping member using dial gauge, respectively. Figure 18 shows the experimental and calculation results of the spring constant. Figure 18-a) shows the spring constant of measurement stud and hub, and Fig. 18-b) shows the spring constant of set bolt and hub used in actual machine.

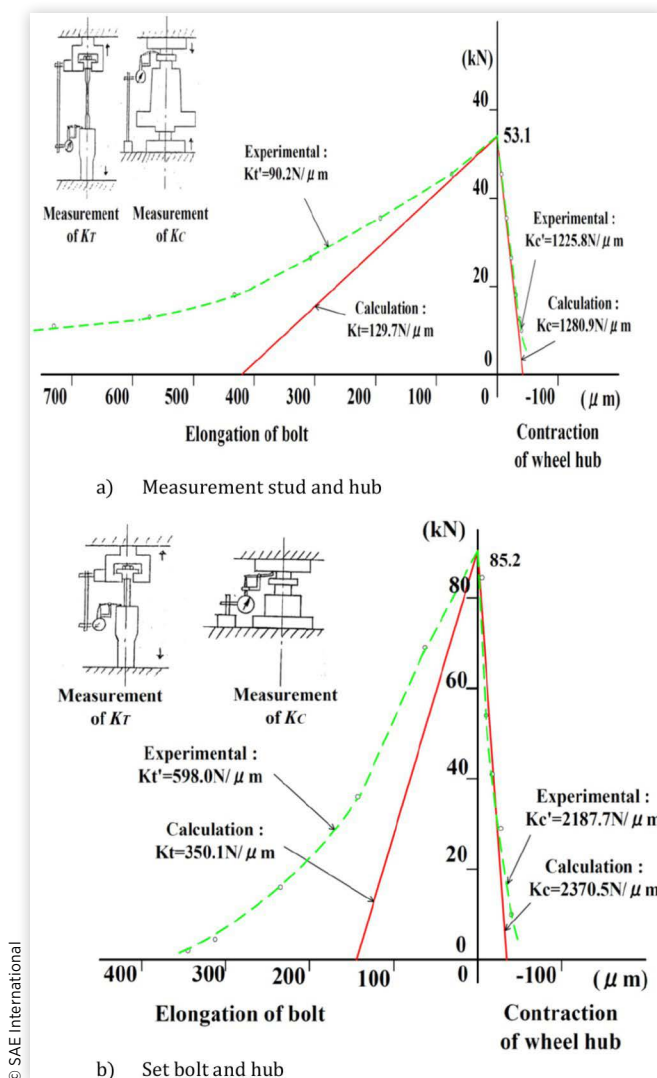
FIGURE 17 Measurement of spring constant (a) Measurement stud and hub (b) Set bolt and hub



© SAE International

© SAE International

FIGURE 18 Experimental results for spring constant



© SAE International

Table 1 shows the calculated and experimentally determined values of stiffness constants and stiffness constant factors of the bolted joint part of a load-measurement stud and an actual bolt of a prototype machine. As reported by Sawa and Omiya [20], the experimentally determined stiffness constants, Φ , are lower than those calculated with the standard equation Φ_T .

TABLE 1 Calculated and experimental data of stiffness constant and stiffness constant factor

Term		Calculation	Experimental	
Stud joint for measuring instrument	Stiffness constant	Stud(N/μm)	129.7	90.2
		Member (N/μm)	1,230.7	1,225.8
		Stiffness constant factor Φ_T	0.092	0.066
Bolted joint for prototype machine	Stiffness constant	Bolt (N/μm)	598.0	350.1
		Member (N/μm)	2,370.3	2,187.9
		Stiffness constant factor Φ_A	0.201	0.138
Stiffness constant ratio Φ_A/Φ_T			2.18	2.09

$$\phi_T = K_T / (K_T + K_C) \quad (11)$$

$$\phi = \left\{ K_T / (K_T + K_C) \right\} (K_C / K_{pt}) \quad (12)$$

Here,

K_T : spring constant for bolt-nut system

K_C : compressive spring constant for clamping member

K_{pt} : tensile spring constant

The bending moment of the bolts in a prototype machine, M_e' , was also empirically characterized using the equation below for easier calculation.

$$M_e = \frac{\Phi_A}{\Phi_T} M_e' \dots \quad (13)$$

The load applied to the measured part as derived by the above-mentioned method must in some cases be converted to the load applied to the weakest part of the bolt, but here, the thus introduced load suggested approximates the load applied to the weakest part of the bolt. The maximum stresses on the weakest part of the bolt are calculated from the loads as follows.

$$\sigma_{\max} = \frac{P}{A_2} + \frac{M_e}{Z_2} \dots \quad (14)$$

Here,

σ_{\max} : Maximum axial (nominal) stress at section of weakest part of bolt

τ_{\max} : Maximum shear stress at section of weakest part of bolt

A_2 : Area of section of weakest part of bolt

Z_2 : Section modulus of weakest part of bolt

I_p : Polar moment of inertia of weakest part of bolt

d_2 : Effective diameter of weakest part of bolt

Strength Estimation

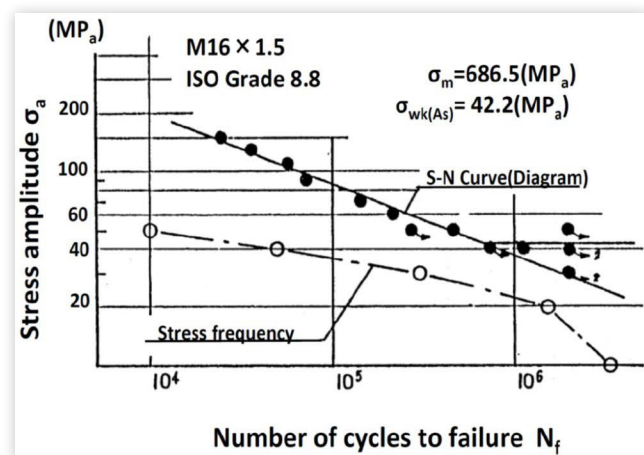
The load frequency diagrams shown in Figs. 9, 13, and 16 are related to the loads applied at an arbitrary section area along the axis of a stud or a bolt. Generally speaking, since the load condition varies along the axis of a stud or a bolt, it is not easy to predict the load condition at a certain section area, such as the weakest section area, from the result of analysis at some other section area.

However, as already mentioned, the structures of most critical bolts of a commercial machine are generally devised and designed so that their load condition is simplified and made uniform. Therefore, in many cases, the load condition at the weakest section area can be estimated by analyzing the load at a certain arbitrary section area. The weakest point of a bolt is generally near where the first thread ridge meshes with the internal thread, and the measured load data here are of practical use for the approximation of the overall load. In this study, it is also considered that the weakest point of a bolt can be derived from the load measured at a point where measurement is practically feasible.

Figure 19 shows the frequency of the occurrence of different levels of stress and the S-N curve of a bolt in a tested machine. To estimate the bolt strength, the lifetime under an operational load is calculated from these results by a fatigue life estimation method. The stress occurrence frequency data in the figure are the results of counting the occurrences of different levels of stress based on the same method as that used to calculate the load peak occurrence frequency and the maximum nominal axial stress with Equation (12) using the time series data of load peak values. The S-N curve was derived by testing an equivalent bolt used in a commercial machine using electrohydraulic servo fatigue testing equipment. Various stresses, as shown in the stress frequency diagram, are plotted in the figure against the number of their occurrences in 5000 h for easier comparison with the S-N curve.

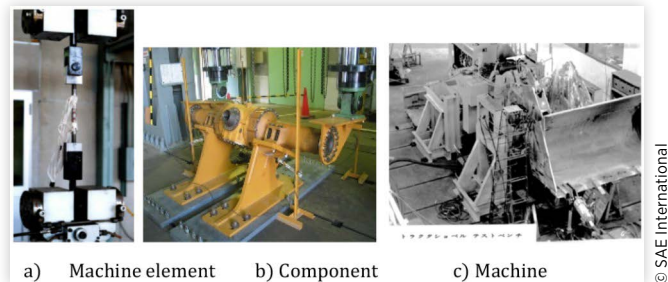
The stress applied to bolts during machine operation is usually designed to be below the fatigue limit, but in such a prototype machine as this example, service stress occasionally exceeds the fatigue limit, as shown in Fig. 19. In such a case, safety is achieved by setting a limited lifetime using a modification of Miner's rule, or the machine is redesigned to reduce the maximum stress to below the fatigue limit. In this example, the bolts shown in Fig. 3-b) were also adopted for commercial machines, and their strength reliability in actual machine operation has been confirmed, as there have been no problems with a machines, which have passed the expected period of endurance.

FIGURE 19 Frequency of stress level occurrence of bolts and S-N curve



© SAE International

FIGURE 20 Photographs taken during of laboratory test in experimental development stage. (a) Machine element b) Component c) Machine



© SAE International

The accuracy of the thus-acquired data of load occurrence frequency and stress occurrence frequency is insufficient due to the inaccuracy of the stiffness constants and measuring positions, but the accuracy can be improved to an industrially acceptable level by standardizing these data based on actual results for commercial products and simple stress measurement using bolt gauges. In particular, a more accurate analysis of stiffness constants may be possible using detailed equations such as the stiffness constant equations derived by Sawa and Omiya [20].

Feedback of Load Analysis and Measurement for Design and Experimental Development Stages

Analysis and measurement results of load affect actual machine use and are feed back to the design and experimental development stages, as shown in the SAE Fatigue Design Handbook [1]. Figure 20 shows photographs taken during an experimental test in a factory laboratory, where the results of load analysis and measurement were used to determine the experimental conditions.

Figure 20 shows the example of machine element, component, and prototype machine test, respectively. Machine element test conditions are determined from the results of load peak frequency analyses (c.f. Figs. 9, 13, and 16). In the component, and prototype machine test, test conditions are determined by the results of a typical working pattern test during cycle of shoveling and dumping operations (c.f. Fig.8), for example.

Conclusions

To estimate the bolted joint strength, it is important to incorporate the measurement and analysis applying loads to bolted

joints into standard technical information for design, which enables the selection of bolts with an appropriate size, strength classification, and configuration. This will lead to the development of fundamental technology for concurrent multiple design, which will be especially effective in promoting efficient product development.

In light of the above, a measurement method using strain gauges and equations for analysis, which derives loads applied to bolted joints, was proposed. Measurement, analysis, and strength estimation were carried out with regard to operational loads applied to the fitting bolts of the base carrier members of a construction machine (wheel loader). The results can be summarized as follows.

(1) Analytical equations for measurements using strain gauges, which calculate loads applied to bolt joints, were proposed, and it was experimentally verified that the axial tension, bending moment, and torsional torque applied to bolts can be separately evaluated with accuracy.

(2) This method was applied to the bolts used to fit the base carrier members of a construction machine, and load peak distribution diagrams were constructed by analyzing the frequency of the occurrence of load peaks of various levels applied to the machine in operation.

(3) A stress distribution diagram was acquired from the time series data of load peaks, and by comparing it with the S-N curve of an equivalent bolt used in a commercial machine, the strength estimation of bolts during machine operation was shown to be possible by a fatigue lifetime estimation method such as a modification of Miner's law.

References

1. Fatigue Design Subcommittee of Division 4 of SAE Iron and Steel Technical Committee, "Fatigue Design Handbook," AE-4, 3-8, 1968.
2. Bickford, J. H., "An Introduction to the Design and Behavior of Bolted Joints (Third Edition)," CRC Press, 213-268, 1995.
3. Bolted Joints Design Committee, *Analysis and Design for Bolted Joints, Japan Research Institute for Screw Threads and Fasteners (JFRI)*, 2016.
4. VDI2230 Blatt 1, "Systematic Calculation of High-duty Bolted Joints (Joints with One Cylindrical Bolts)" (in Japanese), JFRI, 2003.
5. Hareyama, S. and Kodama, S., "A Study on Confidence Limit for Two Independent Probability Variables in Engineering Problems (Applications to Limit of Transmitted Torque in Disk Clutch and Bolt Axial Tension Control)," *JSME International Journal (Series III)* 33(2):256-262, 1990.
6. Hareyama, S., Manabe, K., Nakashima, M., "Improving Tightening Reliability on Bolted Joints for Calibrated Wrench Method (An Analysis on Optimum Tightening Torque by Confidence Limit Ellipse)," Proceedings of ASME 2013 International Mechanical Engineering Congress & Exposition, Vol. 2B: Advanced Manufacturing, IMECE2013-63387, 12 pages, 2013.
7. Hareyama, S., Manabe, K., "Advantage of Elliptical Confidence Limit Method for Bolted Joint Tightening Reliability," Proceedings of ASME, IMECE2015-50729, 10 pages, 2015.
8. Hareyama, S., Manabe, K., Shimodaira, T., Naganawa, T., "Experimental Study to Verify Elliptical Confidence Limit Method for Bolted Joint Tightening," Proceedings of the ASME IMECE2016-66336, 9 pages, 2016.
9. Kumar, R., "Fatigue Life Estimation for Inters in Class 1 Component," *ASME Journal of Pressure Vessel Technology*, February 1998, Vol. 120, 81-85, February 1998.
10. Ellis, F. V., Sielski, D. R., Viswanathan, R., "An Improved Analytical Method for Life Prediction of Bolting," *ASME Journal of Pressure Vessel Technology*, Vol. 123, 71-74, February 2001.
11. Hareyama, S., Manabe, K., Shimodaira, T. and Hoshi, A., "Working Load Analysis and Strength Estimation for Bolted Joints during Actual Machine Operation," Proceedings of ASME, IMECE2014-39193, 10 pages, 2014.
12. Hareyama, S., Manabe, K., Nakashima, K., Shimodaira, T., and Hoshi, A., "Residual Clamping Force Estimation and Lifetime Prediction to Loosening Failure of Bolted Joints," SAE Technical Paper [2017-01-0479](https://doi.org/10.4271/2017-01-0479), 2017, doi:10.4271/2017-01-0479.
13. Junker, G.H. and Williams, D.A., "Rules for Design and Calculation of High-Duty Bolted Joints (Part One: Basic Design)," *Sub Assembly* 11(3):22-24, 1973.
14. Junker, G.H., "New Criteria for Self-Loosening of Fasteners Under Vibration," *SAE Transactions* [690055314](https://doi.org/10.4271/1969-335), 335, 1969.
15. Baggerly, G.R., "Hydrogen-Assisted Stress Cracking of High-Strength Wheel Bolts," *Engineering Failure Analysis* 3(4): 231-240, 1996.
16. Fukuoka, T., Nomura, M., Kamihira, T., "Finite Element Analysis of the Cyclic Stress Amplitude of Wheel Bolts for Large Vehicles" (in Japanese)," *Transactions of the Japan Society of Mechanical Engineers*, Vol. 77, No. 782, 3840-3849, 2011.
17. JFRI Committee for Research of Bolt Tightening, "Research on Tightening Characteristics of High Strength Bolts (Report 1)" (in Japanese), JFRI, 79, 1978.
18. Weber, J.O., Berger, C., and Arz, U., "Nut Resilience and Vibration Fatigue Limit of Bolted Joints," SAE Technical Paper Series [SAE-2008-01-05447](https://doi.org/10.4271/2008-01-05447), 2008.
19. Minguez, M.J. and Vogwell, J., "Effect of Torque Tightening on the Fatigue Strength of Bolted Joints, Engineering Failure Analysis," 13(8):1410-1421, 2006.
20. Sawa, T., Omiya, Y., "New Design Formula for Bolted Joints Under Tensile Loads," Proceedings of ASME 2013 International Mechanical Engineering Congress & Exposition, Vol. 2B: Advanced Manufacturing, IMECE2013-65150, 10 pages, 2013.

Contact Information

Mr. Soichi Hareyama, Dr. Eng.
Visiting Researcher and Part-time Lecturer,
Tokyo Metropolitan University, Japan
hare-lab@ivy.ocn.ne.jp,
hareyama-soichi@tmu.ac.jp.

Moreover, the results of outstanding research by many researchers and engineers have provided us with many helpful suggestions. We deeply appreciate their cooperation and pioneering research.

Acknowledgments

We would not have been able to carry out this study without the cooperation of UniCarriers Corporation, Hitachi Construction Machinery, and Hardlock Industry Co., Ltd.